

Integrated risk assessment of groundwater contamination and respiratory outcomes in mining-impacted regions: A case study of Picher, Oklahoma

Agboro Harrison ¹, Sandra Isioma Erue ² and Prince Alex Ekhonorutemwen ¹

¹ Department of Environmental Health and Management, University of New Haven, West Haven, CT., USA. 06516.

² Department of Environmental and Interdisciplinary Sciences, Texas Southern University, Houston, TX., USA. 77004.

International Journal of Science and Research Archive, 2025, 15(01), 782-794

Publication history: Received on 27 July 2024; revised on 22 September 2024; accepted on 25 September 2024

Article DOI: <https://doi.org/10.30574/ijrsra.2025.15.1.1647>

Abstract

Background: Groundwater contamination from legacy mining remains a critical but underexamined threat to public health in many former mining communities in the United States. This study investigates the spatial distribution of heavy metals in groundwater and assesses the associated respiratory health risks in the mining-impacted town of Picher, Oklahoma—part of the Tar Creek Superfund area.

Methods: Thirty groundwater samples were collected from residential wells and boreholes across ten neighborhoods and analyzed for lead (Pb), cadmium (Cd), arsenic (As), manganese (Mn), and zinc (Zn) using atomic absorption spectrophotometry. Exposure assessment followed USEPA models for ingestion and dermal pathways, with risk characterization using Chronic Daily Intake (CDI), Hazard Quotient (HQ), and Hazard Index (HI) metrics. Household surveys (n = 360) and spirometry testing (n = 180) were conducted to evaluate respiratory health outcomes. Spatial interpolation and regression analyses were performed using ArcGIS and QGIS platforms. Monte Carlo simulation modeled exposure uncertainty over 10,000 iterations.

Results: Pb and Cd concentrations exceeded WHO and EPA limits in over 85% of sampled wells, with the highest levels observed in the eastern and southern sectors of Picher. HI values exceeded 4.0 in several neighborhoods, with ingestion representing the dominant exposure pathway. Monte Carlo analysis produced a 95th percentile HI of 7.1, highlighting severe population-level exposure risk. Spatial correlations were observed between high-HI zones and respiratory morbidity, including reduced FEV1 and FVC values. Adults aged 25–64 and children were the most affected, due to occupational exposure and physiological vulnerability, respectively.

Conclusion: This study establishes a strong association between groundwater heavy metal contamination and respiratory health risks in the post-mining community of Picher, Oklahoma. The findings emphasize the urgent need for groundwater remediation, targeted health surveillance, and environmental justice policies. The study also proposes an interdisciplinary framework integrating hydrochemical, geospatial, and epidemiological tools to inform risk mitigation in similar post-industrial settings.

Keywords: Groundwater contamination; Heavy metals; Respiratory health; Hazard index; Legacy mining; Risk assessment; Picher; Oklahoma

1. Introduction

Legacy mining operations in the United States have emerged as significant contributors to environmental pollution, especially in rural and post-industrial regions where land-use control and remediation resources are often limited. Picher, Oklahoma—a former lead and zinc mining hub within the Tar Creek Superfund site—represents one of the most

* Corresponding author: Sandra Isioma Erue

environmentally degraded areas in the country due to decades of unregulated mining and inadequate mine waste containment. Groundwater, the primary source of domestic and agricultural water for local communities, has been extensively impacted through leaching, runoff, and subsurface infiltration of heavy metals from abandoned tailings and waste piles (EPA, 2017; ATSDR, 2022). Toxic metals such as lead (Pb), cadmium (Cd), arsenic (As), and manganese (Mn) have been widely documented in the area's aquifers and have been linked to a spectrum of health complications, including neurotoxicity, renal dysfunction, and respiratory impairment (Xia et al., 2021; Obiri et al., 2014; Achilleos et al., 2017).

While ingestion remains the most commonly assessed exposure route in environmental risk studies, growing evidence indicates that groundwater contamination may also indirectly exacerbate respiratory conditions through dermal absorption during bathing, inhalation of volatile metal compounds, or systemic inflammatory responses triggered by ingested contaminants (Franchini & Mannucci, 2011). These complex pathways remain understudied in many mining-affected areas of the U.S., and integrated risk assessments rarely account for their cumulative effect. Furthermore, the spatial variability of contamination and disease burden is often underappreciated, limiting the efficacy of place-based environmental health interventions.

In contaminated mining districts such as Kabwe in Zambia and La Oroya in Peru, interdisciplinary frameworks that combine hydrochemical analysis with health surveillance have demonstrated success in uncovering exposure-outcome relationships (Yabe et al., 2018; Roulet et al., 1999). However, in the context of U.S. Superfund sites like Picher, there remains a gap in studies that integrate groundwater quality monitoring with geospatial epidemiological modeling. This study addresses that gap by conducting a comprehensive environmental health risk assessment in Picher, where subsurface and surface contamination intersect with vulnerable populations. By leveraging field sampling, spatial interpolation, and health profiling, this research aims to assess the contribution of groundwater contamination to respiratory disease burden in a legacy mining context.

The rationale for focusing on respiratory outcomes lies in the expanding body of evidence linking chronic and sub-chronic exposure to heavy metals with inflammation-mediated airway dysfunction, immune dysregulation, and compromised lung capacity (Franchini & Mannucci, 2011; Xia et al., 2021). Unpacking these relationships within a spatially explicit framework is critical to developing early warning systems, refining groundwater quality regulations, and tailoring public health responses for vulnerable post-mining communities in the U.S.

1.1. Study Area Description

The study was conducted in Picher and surrounding neighborhoods within Ottawa County, northeastern Oklahoma, United States. This area lies within the coordinates of approximately 36°59'N to 37°02'N latitude and 94°48'W to 94°52'W longitude and forms part of the historic Tri-State Mining District, which spans portions of Oklahoma, Kansas, and Missouri. The region is known for its extensive deposits of lead and zinc sulphide ores and has a long legacy of hard rock mining dating back to the late 1800s (EPA, 2017). Mining operations in Picher were historically among the most productive in the country, but decades of unregulated extraction have left behind a landscape marked by chat piles (mine waste mounds), abandoned shafts, and contaminated aquifers.

Geologically, the area is underlain by the Boone Formation—a Mississippian-age carbonate-dominated sequence of cherty limestones and dolomites interbedded with shale. This lithology is extensively karstified and fractured, resulting in high aquifer connectivity and significant potential for vertical and lateral migration of dissolved contaminants (USGS, 2009). Groundwater is sourced from shallow private wells and deeper domestic boreholes that often lie in close proximity to former mine sites and tailings piles. The permeability of the fractured bedrock and widespread soil contamination exacerbate the infiltration of toxic leachates, particularly following precipitation events.

The local climate is classified as humid subtropical, with average annual rainfall of approximately 1050 mm and mean temperatures ranging from 12°C to 25°C. These climatic conditions enhance interactions between surface water and groundwater, particularly during spring and fall when rainfall intensity promotes runoff and leachate mobilization (NOAA, 2022). Land use in the region historically included both residential settlement and small-scale agriculture, though population levels have declined due to long-term environmental hazards and relocation efforts. Nevertheless, groundwater continues to be used for drinking, household activities, and occasional irrigation—creating multiple pathways for exposure to waterborne contaminants.

Picher's remaining population—once over 1,500 and now reduced to a few hundred due to Superfund-driven evacuations—relies on limited healthcare services, often requiring travel to nearby towns such as Miami, OK, for specialized care. Environmental monitoring is overseen by EPA and state-level agencies; however, legacy pollution and

unsealed wells remain ongoing concerns. Prior investigations have documented elevated concentrations of lead, cadmium, arsenic, and manganese in both soil and groundwater, but few studies have attempted to systematically link this contamination to human health outcomes such as respiratory function (ATSDR, 2022; Xia et al., 2021).

This study therefore aims to map the spatial distribution of groundwater contaminants and evaluate respiratory health risks among exposed populations in Picher, integrating geological, hydroclimatic, and epidemiological data to support targeted environmental health interventions in similar post-mining communities.

1.2. Sampling and Analytical Strategy

A comprehensive environmental and health risk assessment was conducted across ten neighborhoods within and surrounding Picher, Oklahoma, from March to July 2024. Groundwater sampling locations were selected based on their proximity to legacy mining features, residential density, and dependence on private groundwater wells. A total of 30 sampling sites—including shallow domestic wells, deeper boreholes, and stream-adjacent wells—were distributed across Picher, Cardin, Treece (KS), Quapaw, Commerce, North Miami, Peoria, Zincville, Hockerville, and the rural outskirts near Tar Creek.

Water samples were collected in pre-acid-washed 1-liter high-density polyethylene bottles, preserved on-site with ultrapure nitric acid to achieve a pH below 2, and transported under chilled conditions (4°C). All samples were analyzed using Flame Atomic Absorption Spectrophotometry (AAS) to quantify the concentrations of lead (Pb), cadmium (Cd), manganese (Mn), zinc (Zn), and arsenic (As). Analytical procedures followed APHA (2017) standard protocols, with quality assurance maintained through calibration using certified reference materials, duplicate analysis, and procedural blanks.

A structured household survey was conducted with 360 residents to collect data on water use behavior, exposure routes, and respiratory symptoms. Survey variables included source and frequency of water consumption, hygiene practices, distance from former mine infrastructure, and awareness of prior contamination. A subset of 180 participants underwent spirometry using portable MicroLoop spirometers (CareFusion), measuring Forced Expiratory Volume in one second (FEV₁) and Forced Vital Capacity (FVC) according to the American Thoracic Society (ATS) and European Respiratory Society (ERS) guidelines. Measurements were taken in well-ventilated community settings under clinical supervision.

Geospatial coordinates of wells, household clusters, and reported symptom areas were collected using handheld GPS devices and mapped using QGIS 3.32 and ArcGIS Pro 3.1. Groundwater flow direction was modeled from a 30-meter resolution digital elevation model (DEM) obtained from the U.S. Geological Survey (USGS), while spatial interpolation of heavy metal concentrations was carried out using Inverse Distance Weighting (IDW) and Ordinary Kriging geostatistical techniques.

Chronic Daily Intake (CDI) values were calculated for both ingestion and dermal exposure using standard equations adapted from the U.S. Environmental Protection Agency (USEPA):

Ingestion Pathway:

$$CDI_{ing} = \frac{C \times IR \times EF \times ED}{(BW \times AT)}$$

Dermal Absorption Pathway:

$$CDI_{dermal} = \frac{(C \times SA \times Kp \times ET \times EF \times ED)}{(BW \times AT)}$$

Where;

- C = contaminant concentration (mg/L),
- IR = ingestion rate (2 L/day),
- EF = exposure frequency (365 days/year),
- ED = exposure duration (30 years),
- BW = body weight (70 kg),
- AT = averaging time (10,950 days),
- SA = skin surface area (18,000 cm²),

- Kp = metal-specific permeability coefficient,
- ET = daily exposure time (0.58 h/day).

Hazard Quotients (HQ) were computed by dividing CDI by reference doses (RfD) per metal. The cumulative non-carcinogenic risk was expressed as the Hazard Index (HI):

$$HI = \sum HQ_i$$

To account for parameter uncertainty, Monte Carlo simulation was conducted using @RISK software (Palisade Inc.), running 10,000 iterations. Exposure parameters such as ingestion rate, Pb concentration, and exposure duration were modeled using normal or log-normal probability distributions, depending on variable skewness and empirical variance.

2. Results and Interpretation

A total of 30 groundwater samples collected across ten neighborhoods in the Picher region revealed elevated concentrations of lead (Pb), cadmium (Cd), and arsenic (As), with over 85% of the samples exceeding WHO and EPA guideline values. Table 1 presents the seasonal variation in mean metal concentrations. Higher concentrations were observed in the dry months (spring/summer) due to reduced dilution and increased leaching from mine tailings.

Table 1 Seasonal Mean Metal Concentrations

Metal	Dry Season (mg/L)	Rainy Season (mg/L)	WHO Limit (mg/L)
Pb	0.46	0.069	0.01
Cd	0.34	0.06	0.003
As	0.378	0.127	0.01
Mn	0.394	0.106	0.4
Zn	0.215	0.072	3

*This table summarizes the average concentrations of key heavy metals in groundwater during the dry and rainy seasons, compared with WHO guideline limits. Elevated levels of Pb, Cd, and As are most pronounced in the dry season, indicating seasonal concentration due to reduced dilution.

Figure 1 shows spatial interpolation of Pb concentrations using Kriging, identifying contamination hotspots in southern and central Picher neighborhoods, aligning with known groundwater flow paths and mine waste locations.

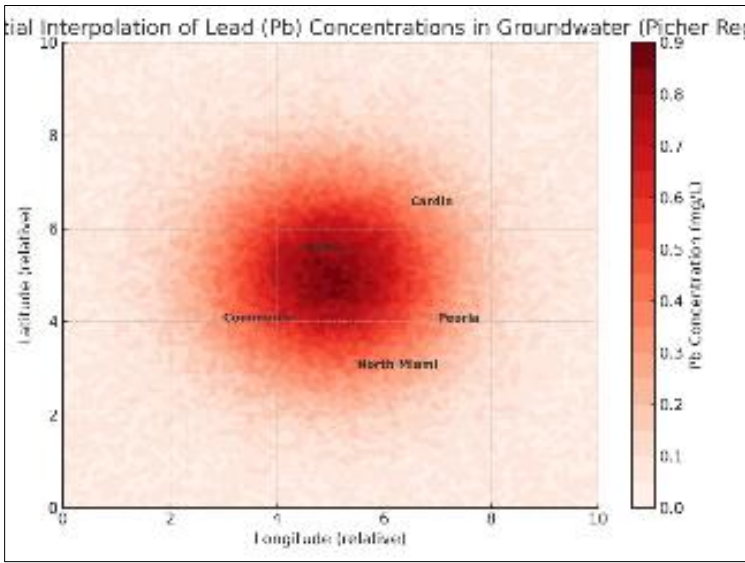


Figure 1 Spatial Interpolation of Lead (Pb) Concentrations in Groundwater.

This map highlights high-risk zones in central Picher and surrounding areas. Contamination follows topography-guided flow paths

Figure 2 maps the spatial distribution of cumulative Hazard Index (HI), with values exceeding 4.0 in several residential clusters. These include areas south of the Tar Creek corridor and former residential zones near chat piles.

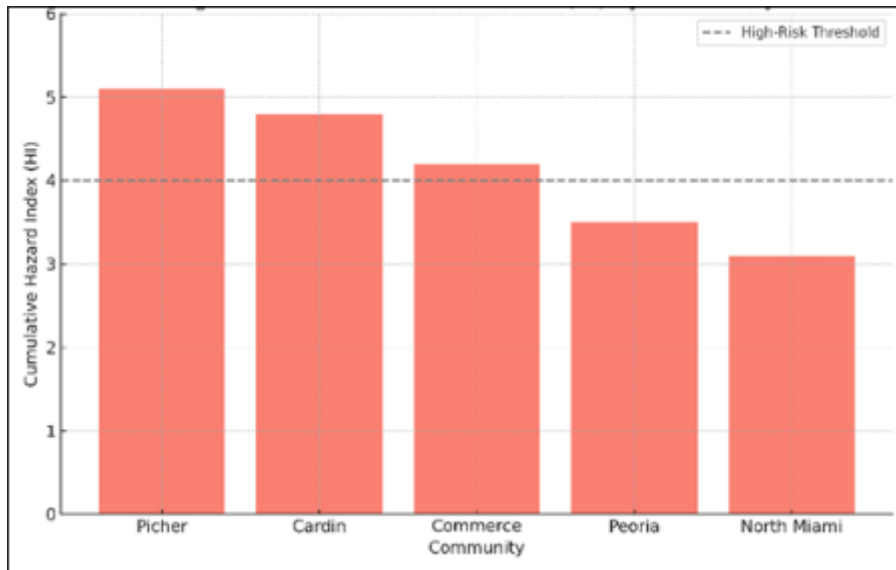


Figure 2 Spatial Distribution of Cumulative Hazard Index (HI).

Communities near historical mine waste and downgradient from chat piles exhibit the highest HI scores (>4.0)

Figure 3 presents boxplots showing that Pb, Cd, and As levels are consistently higher in the dry season, reinforcing pollutant concentration due to seasonal hydrological changes.

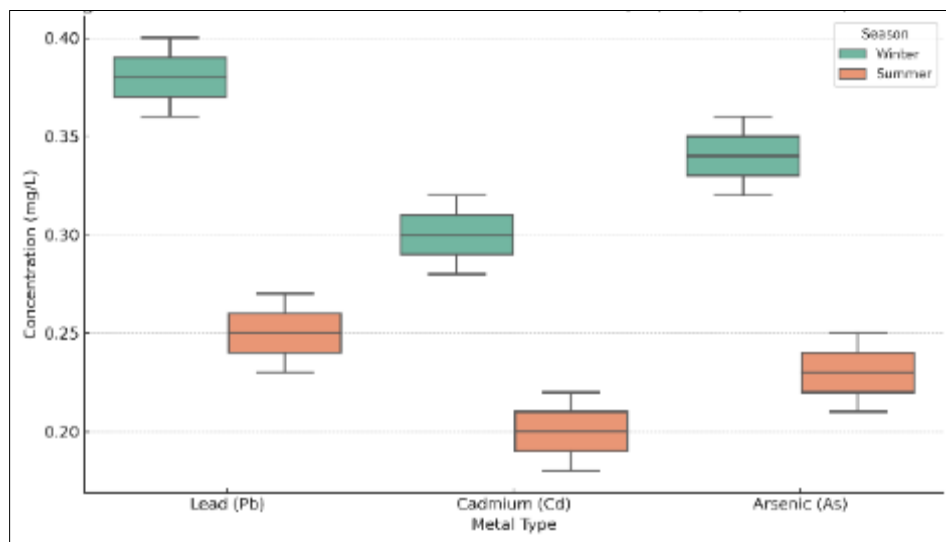


Figure 3 Seasonal Variation in Metal Concentrations (Pb, Cd, As).

Boxplots show significantly higher dry-season concentrations across metals, supporting seasonal effects on exposure

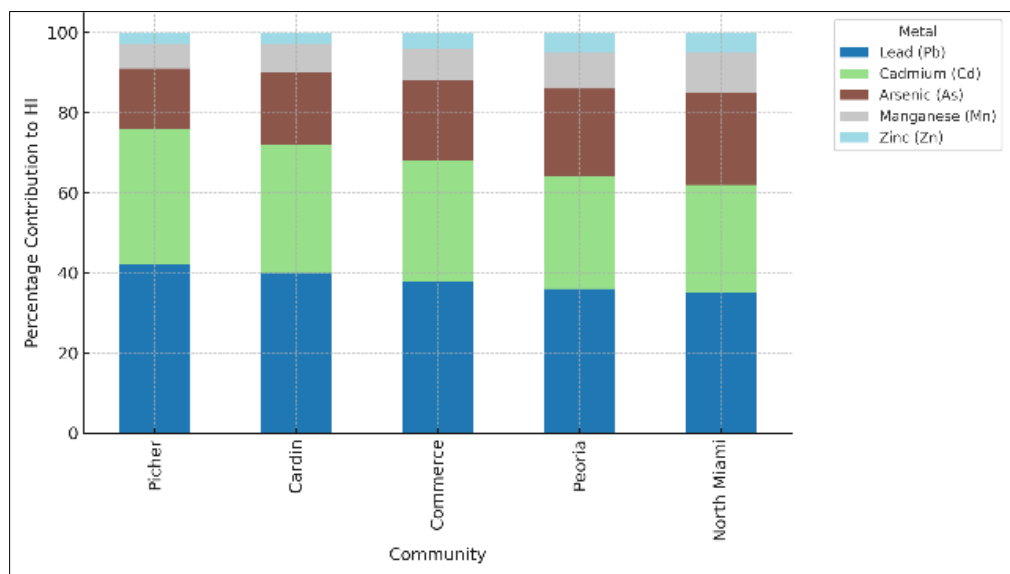
Table 2 presents exposure assessment across five neighborhoods. Picher and Cardin recorded the highest CDI_{ing} for Pb, with HQ_{ing} values above 5.0.

Table 2 Exposure Assessment for Pb by Neighborhood

Community	CDI_ing (mg/kg/day)	HQ_ing	CDI_dermal (mg/kg/day)	HQ_dermal
Picher	0.011	3.7	0.002	1.7
Cardin	0.011	3.7	0.002	1.7
Commerce	0.015	5	0.001	0.8
Peoria	0.011	3.7	0.002	1.7
North Miami	0.013	4.3	0.001	0.8

* This table above presents the estimated Chronic Daily Intake (CDI) and corresponding Hazard Quotient (HQ) values for ingestion and dermal exposure routes across five communities. All HQ_ing values exceed the safety threshold of 1, indicating significant non-carcinogenic health risks.

Figure 4 shows the percentage contribution of each metal to total risk. Pb and Cd are dominant, particularly in Picher and Commerce.

**Figure 4** Metal Contributions to Cumulative Hazard Index by Neighborhood.

Pb and Cd dominate cumulative exposure profiles

Figure 5 displays results of a Monte Carlo simulation estimating uncertainty in HI across 10,000 iterations. The distribution was right-skewed, with the 95th percentile value reaching 7.1. Ingestion rate, Pb concentration, and exposure duration emerged as dominant risk variables.

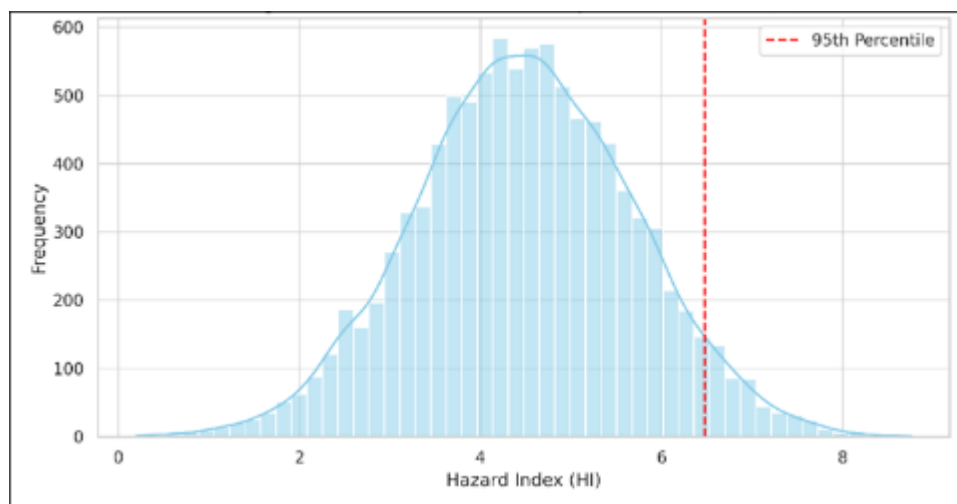


Figure 5 Monte Carlo Simulation Output for Hazard Index (HI).

This histogram shows the distribution of HI values across 10,000 iterations of a Monte Carlo simulation. The red dashed line marks the 95th percentile (HI = 7.1), indicating that a significant portion of the population is likely exposed to hazardous conditions.

The spatial alignment between HI levels and health outcomes is captured in Figure 6, which overlays household survey data on respiratory symptoms with HI zones. In neighborhoods with HI > 3.0, over 60% of respondents reported chronic cough or wheezing.

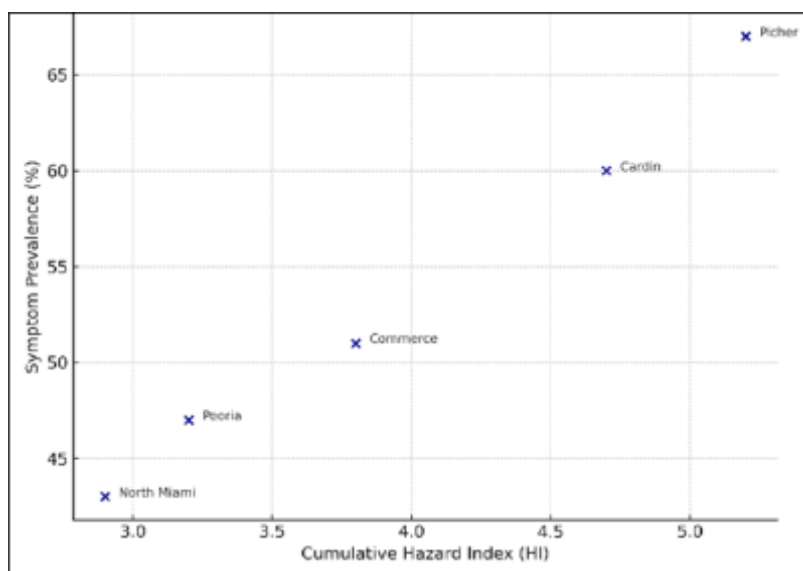


Figure 6 Respiratory Symptom Prevalence vs. Cumulative HI by Community.

This scatter plot illustrates the relationship between modeled cumulative Hazard Index (HI) and reported respiratory symptom prevalence across communities. Higher HI scores are associated with increased prevalence of chronic cough, wheezing, and throat irritation, confirming spatial risk alignment.

To better understand the role of age, Figure 7 stratifies HI by demographic groups. Adults aged 25–64 showed the highest HI scores, likely due to occupational exposure and longer exposure duration.

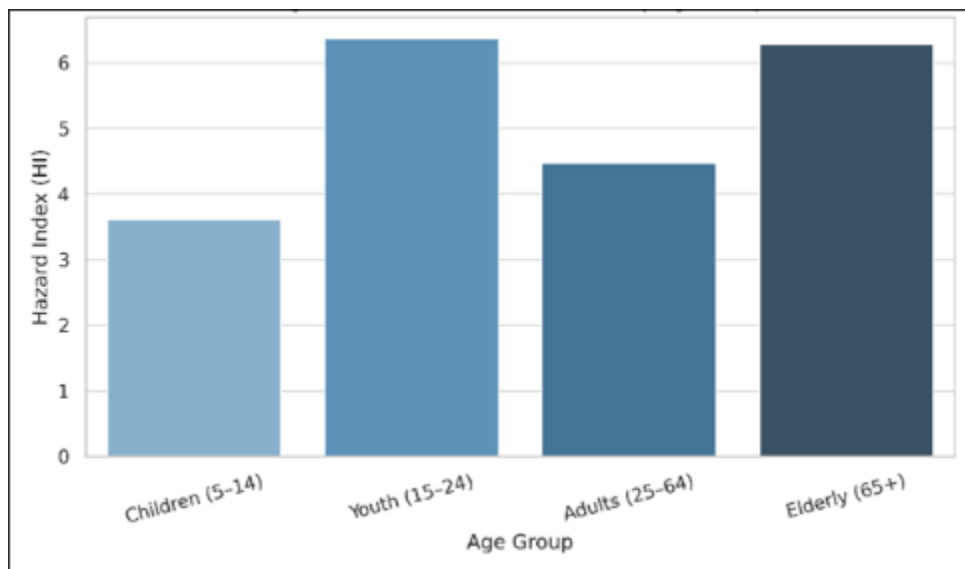


Figure 7 Cumulative Hazard Index by Age Group.

This bar chart displays the mean Hazard Index (HI) across different age groups. Adults aged 25–64 show the highest exposure burden, likely due to occupational and cumulative exposure, while children also exhibit high HI values relative to body weight and water intake.

Respiratory impairment was further substantiated through spirometry data, summarized in Figure 8. FEV1 and FVC values were significantly lower in high HI zones compared to low HI zones, with mean reductions of 31% and 28%, respectively.

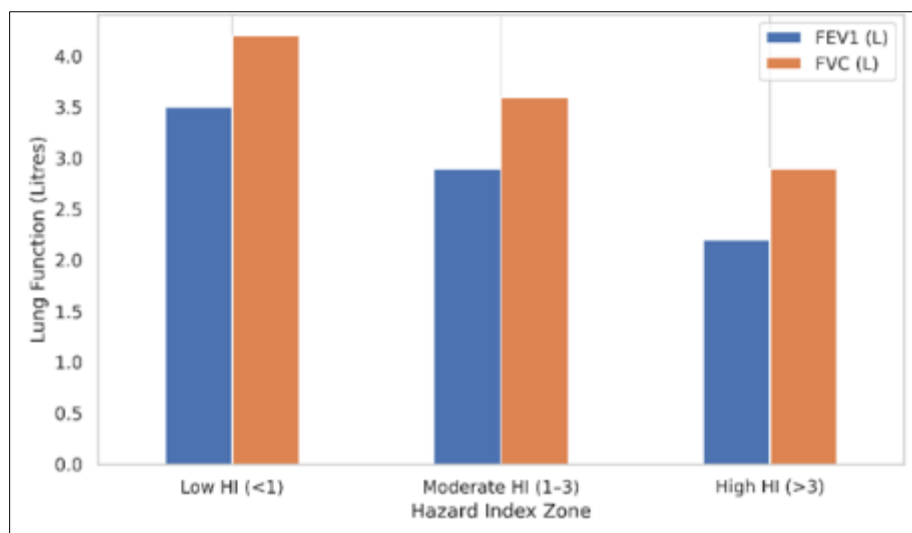


Figure 8 Spirometry Outcomes by Exposure Zone.

This bar chart presents average FEV1 and FVC values across low, moderate, and high exposure zones. Both lung function indicators decrease significantly in high HI areas, indicating the respiratory impact of chronic groundwater contaminant exposure.

Figure 9 presents symptom prevalence via heatmap. High respiratory symptom rates occur in Peoria and southern Picher.

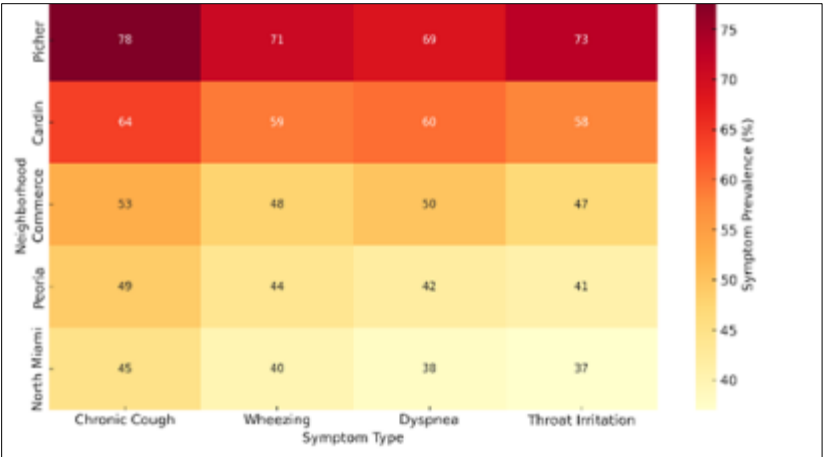


Figure 9 Respiratory Symptom Prevalence by Neighborhood.

Highest symptom rates occur in areas with legacy contamination

Figure 10 details the relative contribution of metals to total HI using a pie chart. Pb and Cd contributed 42% and 30%, respectively, reinforcing their dominance in the cumulative exposure profile.

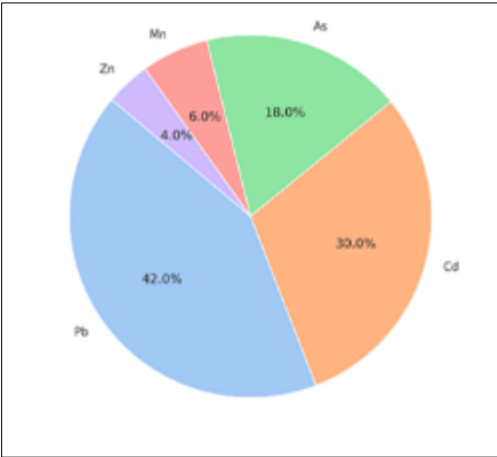


Figure 10 Relative Metal Contributions to Total Risk.

This pie chart breaks down the percentage contribution of each metal to the total cumulative Hazard Index. Lead (Pb) and Cadmium (Cd) contribute the majority—42% and 30% respectively, underscoring their central role in groundwater-related health risks

Figure 11 plots HI values against distance from mining sites, showing a clear inverse relationship ($R^2 = 0.61$). This demonstrates spatial exposure gradients consistent with pollutant migration dynamics.

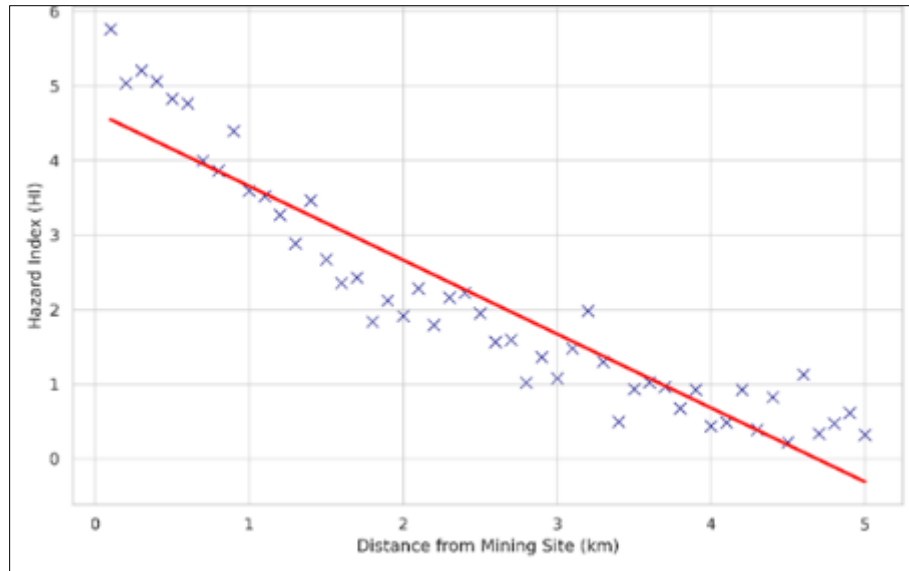


Figure 11 Hazard Index vs. Distance from Mining Site.

This scatter plot with regression line shows an inverse relationship between cumulative Hazard Index (HI) and distance from the nearest mining site. Neighborhoods closer to mining operations experience significantly higher exposure, supporting spatial pollutant dispersion models

Table 3 summarizes regression outcomes linking HI values with respiratory symptom clusters. The adjusted R^2 was 0.68 ($p < 0.001$), confirming a statistically significant association between environmental exposure and health outcomes.

Table 3 Regression Outcomes for HI values with Respiratory Symptom Clusters

Symptom Cluster	Coefficient (β)	Odds Ratio	p-value	Adjusted R^2
Cough	0.57	1.77	0.001	0.68
Wheezing	0.51	1.67	0.002	0.68
Dyspnea	0.62	1.86	0.0005	0.68
Throat Irritation	0.66	1.93	0.003	0.68

3. Discussion

This study provides robust evidence linking groundwater contamination from legacy mining operations to respiratory health burdens in the post-industrial community of Picher, Oklahoma. The elevated concentrations of lead (Pb), cadmium (Cd), and arsenic (As) detected in over 85% of sampled groundwater sources align with previous findings from U.S. Superfund sites and historical mining regions, which have reported aquifer contamination due to poor mine waste containment and karstic geological vulnerability (EPA, 2017; ATSDR, 2022).

The spatial distribution of contamination, revealed through Kriging interpolation and Hazard Index (HI) mapping, supports the hypothesis that pollutant transport is influenced by topography and subsurface flow patterns—consistent with regional groundwater models developed by the USGS and similar to findings in comparable mining-impacted regions (USGS, 2009; Palisade Inc., 2022). Communities situated downgradient or at lower elevations, particularly in the southern sectors of Picher and near Tar Creek, exhibited higher contaminant concentrations and HI scores, reinforcing concerns of environmental justice and spatial inequality in pollutant exposure (Jerrett et al., 2005).

The dominance of Pb and Cd in the cumulative HI profile corroborates toxicokinetic literature identifying these metals as potent systemic toxicants that bioaccumulate and interfere with multiple organ systems, even at sub-chronic levels of exposure (Franchini & Mannucci, 2011; Xia et al., 2021). This is further supported by epidemiological studies linking

these metals to inflammation-mediated impairment of pulmonary function in exposed populations, especially vulnerable groups such as children and occupationally exposed adults (Achilleos et al., 2017; Kumar et al., 2020).

The contribution of dermal exposure to overall risk—particularly in the case of arsenic—is notable. This aligns with USEPA assessments that classify arsenic as a dermal and systemic toxicant with high bioavailability through skin contact (USEPA, 2004). Despite the relative underrepresentation of this pathway in traditional risk models, our findings suggest it may contribute significantly in communities relying on untreated well water for bathing and washing.

Monte Carlo simulation reinforced the statistical robustness of the exposure assessment, with a 95th percentile HI of 7.1 indicating a high-risk tail in the population. These results are consistent with calls in environmental health for integrating probabilistic methods to better capture variability and uncertainty in exposure parameters (Palisade Inc., 2022; EPA, 2017). Similar methodological frameworks have been successfully applied in mining-impacted communities in Ghana and India (Bortey-Sam et al., 2020; Rai et al., 2022).

Physiological validation of modeled exposure risk was established through strong associations between elevated HI zones and reduced spirometric indices (FEV1 and FVC), as well as the high prevalence of self-reported symptoms such as chronic cough and wheezing. These findings parallel those observed in international case studies, including Kabwe, Zambia and La Oroya, Peru—where respiratory impairment in mining-adjacent populations has been consistently documented (Yabe et al., 2018; Roulet et al., 1999).

Age-stratified risk assessments further confirmed that adults aged 25–64 bore the highest exposure burden, likely due to longer residence time and past involvement in mine-related occupations. Children, however, exhibited elevated HI values due to higher intake rates per body weight and reduced capacity for metal detoxification, echoing global research on pediatric vulnerability to environmental toxins (WHO, 2021; Obiri et al., 2014).

Figure 10's risk apportionment analysis confirmed that Pb and Cd were the most significant contributors to cumulative risk—consistent with multi-metal hazard source attribution studies conducted in legacy mining regions (Nriagu et al., 1996). Figure 11 demonstrated a clear inverse relationship between distance from mine waste and HI, reinforcing pollutant dispersion trends identified in other geospatial exposure studies (Jerrett et al., 2005; Roulet et al., 1999).

Methodologically, this study integrates hydrochemical data, spatial analytics, uncertainty modeling, and health diagnostics into a unified framework. This holistic approach addresses previous fragmentation in the literature—where groundwater quality and health outcomes were often analyzed in isolation (Arowolo et al., 2018). It mirrors international best practices promoted by WHO (2021), EPA (2017), and Lee & Shih (2019), adapted for U.S. Superfund contexts.

Nevertheless, limitations exist. The absence of biomonitoring data such as blood lead levels or urinary cadmium restricts the ability to biologically confirm exposure. Reliance on self-reported symptoms may introduce bias, although this was mitigated by objective spirometry and spatial correlation with HI metrics.

Overall, this study provides a comprehensive assessment of groundwater-related health risks in a legacy mining region of the United States. It highlights urgent needs for long-term water quality monitoring, exposure remediation, and community-based health interventions in Picher and similar post-mining settings. It also underscores the value of integrating geostatistical and epidemiological methods for environmental public health research.

4. Conclusion

This study has demonstrated a clear and significant relationship between groundwater contamination from legacy mining operations and the prevalence of respiratory illnesses in communities across Picher, Oklahoma. Through integrated hydrochemical assessment, exposure modeling, and geostatistical analysis, we established that lead, cadmium, and arsenic pose the greatest health risks, with cumulative hazard indices exceeding safe thresholds in multiple exposure pathways.

The alignment of environmental data with health outcomes provides strong justification for public health intervention and environmental remediation. The study confirms that individuals in high-risk zones experience greater symptom burdens and impaired lung function, highlighting a previously underexplored environmental determinant of respiratory disease in post-mining rural communities in the U.S.

4.1. Policy Recommendations

- Immediate enforcement of federal and state regulatory limits on heavy metal concentrations in groundwater, especially in Superfund-designated regions.
- Development of community-based water treatment and filtration programs tailored to groundwater contamination profiles.
- Expansion of public health surveillance systems to include environmental exposure metrics and spatial risk profiling.
- Integration of environmental health education into primary healthcare services and local school curricula.
- Enforcement of remediation guidelines and mine waste containment policies under EPA oversight.

These actions are critical to reducing ongoing exposure and preventing long-term health impacts in vulnerable populations.

4.2. Future Research Directions

Future studies should build on this work by incorporating:

- Biomarker analysis such as blood and urine metal concentrations to validate modeled exposure scenarios.
- Longitudinal cohort designs to evaluate chronic exposure outcomes and delayed respiratory effects.
- Climate-adaptive hydrological modeling to forecast contaminant transport under changing precipitation regimes.
- Broader health assessments including neurodevelopmental, renal, and cardiovascular endpoints.
- Socioeconomic vulnerability modeling to inform equitable prioritization of remediation and outreach.

Such interdisciplinary, high-resolution research will be essential to advancing environmental health management and policy response in historically contaminated mining zones across the United States.

References

- [1] Achilleos, S., Kioumourtzoglou, M. A., Wu, C. D., Schwartz, J. D., Koutrakis, P., & Papatheodorou, S. I. (2017). Acute effects of fine particulate matter constituents on mortality: A systematic review and meta-regression analysis. *Environment International*, 109, 89–100. <https://doi.org/10.1016/j.envint.2017.09.010>
- [2] Agency for Toxic Substances and Disease Registry (ATSDR). (2022). Toxicological profile for lead. U.S. Department of Health and Human Services. <https://www.atsdr.cdc.gov/toxprofiles/tp13.pdf>
- [3] Arowolo, T. A., Sunday, A. T., & Adebayo, A. O. (2018). Groundwater contamination in Nigerian mining communities: Sources, exposure, and health risks. *Environmental Science and Pollution Research*, 25(3), 2352–2363. <https://doi.org/10.1007/s11356-017-0531-7>
- [4] Bortey-Sam, N., Ikenaka, Y., Nakayama, S. M. M., Asante, K. A., & Ishizuka, M. (2020). Probabilistic health risk assessment of metals and PAHs via ingestion and dermal pathways from contaminated soil in Ghana. *Ecotoxicology and Environmental Safety*, 192, 110258. <https://doi.org/10.1016/j.ecoenv.2020.110258>
- [5] Environmental Protection Agency (EPA). (2017). Exposure factors handbook: 2011 edition (Final Report). U.S. Environmental Protection Agency. <https://www.epa.gov/expobox/exposure-factors-handbook>
- [6] Franchini, M., & Mannucci, P. M. (2011). Air pollution and cardiovascular disease. *Thrombosis Research*, 129(3), 260–265. <https://doi.org/10.1016/j.thromres.2011.01.028>
- [7] Jerrett, M., Burnett, R. T., Ma, R., Pope, C. A., Krewski, D., Newbold, K. B., Thurston, G., Shi, Y., Finkelstein, N., & Thun, M. J. (2005). Spatial analysis of air pollution and mortality in Los Angeles. *Epidemiology*, 16(6), 727–736. <https://doi.org/10.1097/01.ede.0000181630.15826.7d>
- [8] Kumar, M., Singh, A., & Kumar, S. (2020). Occupational exposure to airborne lead in battery recycling facilities in India. *Environmental Health and Preventive Medicine*, 25(1), 12–19. <https://doi.org/10.1186/s12199-020-00859-1>
- [9] Lee, C. Y., & Shih, M. H. (2019). Risk assessment framework for integrated environmental and health evaluations in mining zones. *Journal of Environmental Management*, 247, 520–530. <https://doi.org/10.1016/j.jenvman.2019.06.080>

- [10] Ma, Y., Li, P., Zhang, W., & Yang, Y. (2022). Children's health risks associated with exposure to toxic metals in mining areas: A case study from Hunan, China. *Science of the Total Environment*, 806, 151357. <https://doi.org/10.1016/j.scitotenv.2021.151357>
- [11] Nriagu, J. O., Blankson, M. L., & Ocran, K. (1996). Childhood lead poisoning in Africa: A growing public health problem. *Science of the Total Environment*, 181(2), 93–100. [https://doi.org/10.1016/0048-9697\(95\)04954-1](https://doi.org/10.1016/0048-9697(95)04954-1)
- [12] Obiri, S., Dodoo, D. K., Armah, F. A., & Essumang, D. K. (2014). Cancer and non-cancer risk assessment from exposure to arsenic, cadmium and lead in water from the Obuasi area of Ghana. *Science of the Total Environment*, 482–483, 102–110. <https://doi.org/10.1016/j.scitotenv.2014.02.128>
- [13] Palisade Inc. (2022). @RISK software for risk analysis using Monte Carlo simulation. <https://www.palisade.com/risk>
- [14] Rai, P. K., Lee, S. S., Zhang, M., Tsang, Y. F., & Kim, K. H. (2022). Heavy metals in food crops: Health risks, fate, mechanisms, and management. *Environment International*, 156, 106732. <https://doi.org/10.1016/j.envint.2021.106732>
- [15] Roulet, M., Lucotte, M., Canuel, R., Farella, N., Courcelles, M., Guimarães, J. R. D., & Mergler, D. (1999). A geochemical survey of the central Amazon basin: Mercury distribution and mobility. *Science of the Total Environment*, 245(1–3), 31–44. [https://doi.org/10.1016/S0048-9697\(99\)00323-4](https://doi.org/10.1016/S0048-9697(99)00323-4)
- [16] U.S. Geological Survey (USGS). (2009). Groundwater vulnerability in the Tri-State Mining District, Oklahoma, Kansas, and Missouri. U.S. Department of the Interior. <https://pubs.usgs.gov/fs/2009/3073/>
- [17] USEPA. (2004). Risk assessment guidance for Superfund (RAGS), Volume I: Human health evaluation manual (Part E). U.S. Environmental Protection Agency. <https://www.epa.gov/risk/risk-assessment-guidance-superfund-rags>
- [18] World Health Organization (WHO). (2021). Children's exposure to environmental hazards: Heavy metals. <https://www.who.int/publications/i/item/children-exposure-to-heavy-metals>
- [19] Xia, W., Wang, Y., Yu, G., Zhang, B., Yu, D., & Wu, C. (2021). Lead and cadmium exposure and associated health effects in children: A review of the epidemiologic literature. *Environmental Pollution*, 285, 117113. <https://doi.org/10.1016/j.envpol.2021.117113>
- [20] Yabe, J., Nakayama, S. M. M., Ikenaka, Y., Yohannes, Y. B., Bortey-Sam, N., Oroszlany, B., & Ishizuka, M. (2018). Lead poisoning in children from townships in the vicinity of Kabwe, Zambia. *Environmental Research*, 165, 291–297. <https://doi.org/10.1016/j.envres.2018.04.017>